

THE ARROW OF TIME IN THE COLLAPSE OF COLLISIONLESS SELF-GRAVITATING SYSTEMS: NON-VALIDITY OF THE VLASOV-POISSON EQUATION DURING VIOLENT RELAXATION

LEANDRO BERALDO E SILVA,¹ WALTER DE SIQUEIRA PEDRA,² LAERTE SODRÉ,¹ EDER L. D. PERICO,² AND MARCOS LIMA²

¹*Instituto de Astronomia, Geofísica e Ciências Atmosféricas, Universidade de São Paulo, CEP 05508-090, São Paulo, SP, Brazil*

²*Departamento de Física Matemática, Instituto de Física, Universidade de São Paulo, CP 66318, CEP 05314-970, São Paulo, SP, Brazil*

Submitted to ApJ

ABSTRACT

The collapse of a collisionless self-gravitating system, with the fast achievement of a quasi-stationary state, is driven by violent relaxation, with a typical particle interacting with the time-changing collective gravitational potential. It is traditionally assumed that this evolution is described by the (time-reversible) Vlasov-Poisson equation, in which case entropy must be conserved. We use N-body simulations to follow the evolution of an isolated self-gravitating system, estimating the (fine-grained) distribution function and the corresponding Shannon entropy. We do this with three different codes: NBODY-6 (direct summation without softening), NBODY-2 (direct summation with softening) and GADGET-2 (tree code with softening), for different numbers of particles and initial conditions. We find that during violent relaxation entropy increases in a way that cannot be described by 2-body relaxation as modeled by the Fokker-Planck approximation. On the other hand, the long-term evolution is very well described by this model. Our results imply that the violent relaxation process must be described by a kinetic equation other than the Vlasov-Poisson, even if the system is collisionless. Our estimators provide a general method for testing any proposed kinetic equation. We also study the dependence of the 2-body relaxation time-scale τ_{col} on the number of particles N , obtaining $\tau_{col} \propto \sqrt{N}$, and the dependence of τ_{col} on the softening length ε , which can be fit by a function of the form $\tau_{col} \propto \sqrt{\varepsilon} \cdot e^{c\varepsilon}$, for a fixed number of particles.

arXiv:1703.07363v1 [astro-ph.GA] 21 Mar 2017

1. INTRODUCTION

The derivation of reduced dynamical descriptions of large systems composed of many particles is a central issue in Statistical Mechanics. In such systems, the effect of each individual particle is weak, but the collective action of the particle ensemble generates a nontrivial potential field acting on each and every particle. One thus expects that the state of a system with a large number of identical particles is reflected in the statistical behavior of one typical particle in the system. The large scale dynamics is then governed by a set of autonomous equations describing the evolution of the state of this typical particle¹. In some cases, the effective dynamics emerges in a mathematically rigorous fashion through a scaling limit. One important point to be noted is that the effective macroscopic dynamical equations strongly depend on the particular scaling or regime which is considered: the same (large) system appears differently on different scales. For instance, by considering the same system of Newtonian particles interacting via some well-behaved inter-particle potential, one can arrive at the Boltzmann, Landau, or Vlasov equation, as the effective equation for the “macroscopic” dynamics, depending on the time and space scales, as well as the interaction strength regime considered (Spohn 2011).

In this context, one of the deepest and most debated questions in Physics since the early development of Statistical Mechanics is the emergence of the arrow of time in the evolution of macroscopic systems and how to reconcile it with the time-reversible microscopic laws, being them classical, quantum or relativistic (e.g. Ehrenfest & Ehrenfest 1959; Lebowitz 1993a,b; Goldstein 2001). In other words: how to explain, starting from the time-reversible equations of motion for the constituent particles, the irreversibility expressed by the second law of Thermodynamics for the evolution of the system as a whole?

The first to try to solve this problem was L. Boltzmann in the end of the nineteenth century, introducing the equation which now bears his name and the so-called H-theorem, which is intended to prove the entropy increase from mechanical considerations (Brush 1976). The Boltzmann equation is a particular example of a general class of equations, the transport (or kinetic) equations, which describe the time evolution of the distribution function $f(\vec{r}, \vec{v}, t)$, the probability for

a typical particle to be at position \vec{r} and velocity \vec{v} (Lifshitz & Pitaevskii 1980).

The basic format of a transport equation is

$$\frac{df}{dt} = C[f],$$

and the right-hand side represents the physical process relaxing the system, i.e. driving it to equilibrium, introducing the arrow of time. The main hypothesis behind the use of a transport equation of this form is that the state of the system only depends on its immediately previous state, having no long-term “memory” effects, i.e. that the evolution is Markovian – see Balescu (1975).

In the case of a molecular gas, the process responsible for driving the system to equilibrium is represented by the collisions between molecules. For this reason, $C[f]$ is traditionally called the *collisional term*. However, for systems evolving through non-collisional processes, this name can be misleading: relaxation can in principle also be produced by collective, collisionless processes. Henceforth, whenever we refer to the right-hand side of the transport equation, we call it generically the *relaxation term* and use the notation $(\partial f / \partial t)_X$, the index X referring to the process to which it is associated.

When deriving the relaxation term, one has to introduce statistical hypotheses related to the type of interactions between the constituent particles. In the case of a neutral molecular gas, following Boltzmann one can assume that the interactions are short-range, that each interaction is instantaneous and that it involves only two molecules at a time (binary collisions).

Although this discussion has appeared firstly in the study of molecular gases, it applies to any system composed of many interacting particles. In particular, to the process of collapse of self-gravitating systems and the formation of structures in the universe. A self-gravitating system is composed of N gravitationally bound particles moving in the presence of the gravitational potential created by themselves (Spitzer 1987; Binney & Tremaine 2008; Saslaw 1987; Heggie & Hut 2003). They range from globular clusters, composed of $N \approx 10^5$ stars, to galaxies ($N \approx 10^{11}$ stars) and dark matter halos, composed of a giant number of dark matter particles, whose nature is yet unknown. The study of the macroscopic evolution of these systems is of fundamental importance for many reasons, e.g.: they represent the prototype for any long-range interacting system; understanding their macroscopic evolution helps us to theoretically model (beyond the parametrization of the results from numerical simulations) the quasi-stationary state achieved after the relaxation processes and the main functions characterizing this state, namely the density profile and velocity distribution; these func-

¹ The typical particle can also be called the test particle, although we prefer the former, meaning that it represents the behaviour of the vast majority of the particles.

tions, besides their intrinsic importance as dynamical diagnostics, are also key ingredients for other analyses such as those of dark matter direct and indirect detection experiments.

The main difference between a self-gravitating system and a neutral molecular gas is that gravity is a long-range interaction, thus invalidating all of the assumptions involved in the derivation of the Boltzmann equation for molecular gases² (Prigogine & Severne 1966; Padmanabhan 1990). On the other hand, it is still possible to estimate the time-scale for relaxation of a self-gravitating system due to 2-body processes (long-range “collisions”) as (see Binney & Tremaine 2008)

$$\tau_{col} \propto \frac{N}{\ln \Lambda} \cdot \tau_{cr}, \quad (1)$$

where $\Lambda = b_{max}/b_0$ (the ratio between the maximum and minimum impact parameters of the gravitational scatterings – see §3.2) – and τ_{cr} is the time scale for a typical particle to cross the system, the crossing time, which is also of the same order of the dynamical time scale $\tau_{dyn} = 1/\sqrt{\bar{\rho}G}$, where $\bar{\rho}$ is the mean density and G is the gravitational constant.

In the case of a globular cluster, the collisional relaxation time scale is $\tau_{col} \approx 10^3$ Myr, shorter than its age ($\approx 10^4$ Myr) and we conclude that the apparent equilibrium of these objects has as a plausible mechanism the 2-body relaxation, whose relaxation term can be modeled with the Fokker-Planck approximation – see §3.2.

For galaxies and dark matter halos, given the large number of particles it is possible to show that the 2-body relaxation time-scale is $\tau_{col} \gtrsim 10^{11}$ Myr, many orders of magnitude larger than their ages, and therefore this process is not a plausible mechanism to explain the apparent (both observationally and in N -body simulations) near equilibrium state that can be achieved by these systems. They are thus called *collisionless self-gravitating systems* and are the main focus of this work (we do not consider any dissipative component such as gas or dust).

The process generally accepted as the driver of a collisionless self-gravitating system to a quasi-stationary state is the interaction of the typical particle with the time-changing collective gravitational potential during the first stages of the collapse of the system (King 1962; Hénon 1964; Lynden-Bell 1967). It is therefore a collective effect, in contrast to 2-body relaxation. The time-scale for that relaxation process, according to some the-

oretical arguments (Lynden-Bell 1967; Kandrup 1990) and to results from N -body simulations, is the dynamical time scale, which is orders of magnitude smaller than the age of any self-gravitating system. This process is called *violent relaxation* (Lynden-Bell 1967; Shu 1978; Madsen 1987; Shu 1987; Efthymiopoulos et al. 2007; Bindoni & Secco 2008; Levin et al. 2014).

It is interesting to remember that the relaxation process of a general N -body problem is usually related to the presence of stochastic motions that allow the particles to occupy large regions of phase space and the system to forget the initial conditions, the so-called *chaotic mixing* (Merritt & Valluri 1996). In fact, N -body simulations of galaxy formation have shown evidence of very complex motions in phase space and the fast achievement (in a dynamical time-scale) of a quasi-stationary state – see Merritt (1999) and references therein (see also Kandrup et al. (2003) on the role of chaotic mixing in violent relaxation). This seems to indicate that violent relaxation is a real relaxation process, in the sense that it drives the system irreversibly towards the equilibrium state (see also Kandrup 1990), even though violent relaxation is known to be incomplete, ending before the achievement of thermodynamical equilibrium, which would be described by a Maxwell-Boltzmann distribution (Merritt 1999; Kandrup et al. 1993; Efthymiopoulos et al. 2007). Consequently, the system keeps some correlation with the initial conditions. Thus, when we refer to the equilibrium state generated by violent relaxation, we are actually considering this incompletely relaxed, quasi-stationary state, which generally does not correspond to the full thermodynamical equilibrium.

However, since the 2-body relaxation of a collisionless self-gravitating system during the early stages of the collapse is by definition negligible, it is usually assumed that the relaxation term associated to violent relaxation is zero. In this case, the system’s evolution is described by the equation:

$$\frac{df}{dt} \equiv \frac{\partial f}{\partial t} + \vec{v} \cdot \frac{\partial f}{\partial \vec{r}} - \frac{\partial \phi}{\partial \vec{r}} \cdot \frac{\partial f}{\partial \vec{v}} = 0, \quad (2)$$

where $\phi(\vec{r}, t)$ is the gravitational potential associated to the distribution of typical particles, considered as an external potential for the typical particle: $d\vec{v}/dt = -\nabla\phi$. This equation is generically called the Vlasov equation, which can encompass many different equations, depending on the inter-particle potential involved. For the specific problem discussed in this work, namely the evolution of self-gravitating systems, this equation is called the Vlasov-Poisson equation.

The main problem in describing the system’s evolution with the Vlasov-Poisson equation is that this equa-

² In the case of plasmas, the particles also interact via long-range forces (Coulomb interaction). However, the presence of opposite charges produces an screening effect, the Debye shielding, effectively shortening the interaction range.

tion is time reversible, while it is intended to describe the irreversible evolution driven by violent relaxation. Besides that, there is no mathematically rigorous proof of the validity of the Vlasov-Poisson equation for self-gravitating systems. Note that, for the Vlasov-Poisson initial value problem itself, there are various results (Pfaffelmoser 1992; Schaeffer 1991; Lions & Perthame 1991; Horst 1993) ensuring global existence and uniqueness of weak and strong solutions under fairly general conditions on the initial configuration. A complete review on the mathematical status of the Vlasov equation as an effective dynamical equation for large Newtonian systems is given in §6.

On the other hand, studies based on the numerical integration of the Vlasov-Poisson equation sometimes obtain results comparable to those obtained from N -body simulations (although frequently simulating situations and scales different from those associated to the violent relaxation process), attributing any difference to N -body codes limitations (Yoshikawa et al. 2013; Colombi et al. 2015; Hahn & Angulo 2016).

A possible path to derive the Vlasov-Poisson equation is by means of the so-called BBGKY hierarchy, but this involves the assumption of delicate hypotheses which, in our view, do not have plausible reasons to be valid during violent relaxation – see Beraldo e Silva et al. (2014).

Going back to the general form of the transport equation, we have

$$\frac{df}{dt} \equiv \frac{\partial f}{\partial t} + \vec{v} \cdot \frac{\partial f}{\partial \vec{r}} - \frac{\partial \phi}{\partial \vec{r}} \cdot \frac{\partial f}{\partial \vec{v}} = \left(\frac{\partial f}{\partial t} \right)_X. \quad (3)$$

As for any good relaxation process, the relaxation term is responsible for entropy increase. In fact, following Tremaine et al. (1986), let

$$S = - \int s[f] d^3\vec{r} d^3\vec{v}, \quad (4)$$

where $s[f]$ is some functional of the distribution function f . For example, if $s[f] = f \ln f$ then S is the well-known Shannon entropy associated to the distribution f . Accordingly,

$$\frac{dS}{dt} = - \int \frac{ds}{df} \frac{\partial f}{\partial t} d^3\vec{r} d^3\vec{v} \quad (5)$$

and using the transport equation (3):

$$\begin{aligned} \frac{dS}{dt} &= - \int \frac{ds}{df} \left[\left(\frac{\partial f}{\partial t} \right)_X - \vec{v} \cdot \frac{\partial f}{\partial \vec{r}} + \frac{\partial \phi}{\partial \vec{r}} \cdot \frac{\partial f}{\partial \vec{v}} \right] d^3\vec{r} d^3\vec{v} \\ &= - \int \frac{ds}{df} \left(\frac{\partial f}{\partial t} \right)_X d^3\vec{r} d^3\vec{v} + \\ &\quad + \int \left[\vec{v} \cdot \frac{\partial s}{\partial \vec{r}} - \frac{\partial \phi}{\partial \vec{r}} \cdot \frac{\partial s}{\partial \vec{v}} \right] d^3\vec{r} d^3\vec{v} \\ &= - \int \frac{ds}{df} \left(\frac{\partial f}{\partial t} \right)_X d^3\vec{r} d^3\vec{v}. \end{aligned} \quad (6)$$

In the last passage, we integrate the term $\vec{v} \cdot \partial s / \partial \vec{r}$ firstly in $d^3\vec{r}$ and the term $\partial \phi / \partial \vec{r} \cdot \partial s / \partial \vec{v}$ firstly in $d^3\vec{v}$, using the fact that $s[f] \rightarrow 0$ for $\vec{r}, \vec{v} \rightarrow \infty$.

Thus, if the Vlasov-Poisson equation is valid, i.e. if $(\partial f / \partial t)_X = 0$, then S , and particularly the Shannon entropy, is conserved (see Shu 1978; Tremaine et al. 1986). This is to be expected, since the Vlasov-Poisson equation is time-reversible and reversible processes keep the entropy constant. On the other hand, if the quantity defined by Eq. (4) is not conserved, this is a clear evidence for the non-validity of the Vlasov-Poisson equation and of the emergence of the arrow of time.

The main objective of this work is to test the validity of the Vlasov-Poisson equation during the violent relaxation of collisionless self-gravitating systems. We do this using N -body simulations to estimate the entropy of the system at each time, verifying whether it is conserved. While interesting works on the relaxation of self-gravitating systems focus on characterizing the mixing properties of the evolution by means of e.g. calculating Lyapunov exponents or fundamental frequencies (Merritt & Valluri 1996; Valluri & Merritt 1998; Kandrup & Sideris 2001; Kandrup et al. 2003), the key quantity for the relaxation concept, which may be considered to define it, is the entropy. In this sense, this work go straight to the *relaxation* concept, with less regards to its explanation in terms of *mixing*.

The simulations used here are described in §2, and in §3 we present the estimators used. Then, in §4 we show our results, concluding in §5, with further comments in §6.

In what follows, we will set $s[f] = f \ln f$, i.e. we will only consider the Shannon entropy

$$S = - \int f \ln f d^3\vec{r} d^3\vec{v}. \quad (7)$$

2. N-BODY SIMULATIONS

We use the code NBODY-6 accelerated with a graphics processing unit (GPU) – see Nitadori & Aarseth (2012), which is the result of a long development since

its first version NBODY-1 (Aarseth 1999). It is a direct summation code and the integration is based on the scheme of Ahmad & Cohen (1973) using the forth-order Hermite method (Makino & Aarseth 1992). The code does not make use of a softening in the Newtonian force law, as commonly done to avoid close encounters (see below). Instead, it implements regularization procedures in order to deal with the possible close encounters, binaries and higher-order objects etc. For a general discussion about these techniques, see Aarseth (2003).

We use NBODY-6 to simulate an isolated self-gravitating system with N particles of equal mass m , with initial positions uniformly distributed in a sphere (top-hat initial condition) and with an initial Maxwellian velocity distribution with velocity dispersion determined by the initial virial ratio Q_0 , which is defined as the ratio of kinetic energy T and potential energy U , $Q = T/|U|$. In general, we use as the initial value $Q_0 = 0.5$, which is the value expected for virialized systems. In all simulation runs, the number of escaping particles, when it occurs, is completely negligible. The maximum energy relative error was set to 5×10^{-5} .

Ideally, a N -body simulation code intended to simulate collisionless systems need to run with a (possibly impracticable) large number of particles in order to suppress the 2-body relaxation, at least for the time-scales of interest – see Eq. (1). A widely used strategy is to introduce the softening length parameter ε , modifying the Newtonian gravitational potential to the Plummer-softened one

$$\phi(r) = -\frac{Gm}{\sqrt{r^2 + \varepsilon^2}},$$

and thus avoiding close encounters and suppressing the 2-body relaxation. In order to study the role of the softening length in the relaxation process, we also run the simulation code NBODY-2 (Aarseth 2001) that, differently from NBODY-6, does make use of a softening length. This code is also of direct summation type, but the use of the softening length simplifies the treatment of close encounters in comparison to NBODY-6. Unfortunately, there is no parallelized or GPU accelerated version of NBODY-2, what restricts the possibility of using large numbers of particles.

With the aim of testing the universality of our NBODY-2 and NBODY-6 entropy estimation, we also run the publicly available GADGET-2 code (Springel 2005). GADGET-2 is a hybrid N -body code that combines the traditional evolution of self-gravitating collisionless particles, with the smoothed particle hydrodynamics (SPH) treatment for collisional gas. In our case, we run GADGET-2 using the same initial conditions that were used for NBODY-2 and NBODY-6

simulations, i. e., an isolated set of self-gravitating collisionless particles, within a Newtonian space (without Hubble expansion), and without the presence of any collisional gas. In addition, we run GADGET-2 using its tree configuration, i. e., without using the Fourier techniques to compute long-distance forces.

In order to suppress large-angle scattering during 2-body encounters, the GADGET-2 code uses the spline-softened gravitational potential:

$$\phi(r) = \frac{Gm}{h} W(r/h),$$

where

$$W(u) = \begin{cases} \frac{16}{3}u^2 - \frac{48}{5}u^4 + \frac{32}{5}u^5 - \frac{14}{5}, & 0 \leq u < \frac{1}{2}, \\ \frac{1}{15u} + \frac{32}{3}u^2 - 16u^3 \\ + \frac{48}{5}u^4 - \frac{32}{15}u^5 - \frac{16}{5}, & \frac{1}{2} \leq u < 1, \\ -\frac{1}{u}, & 1 \leq u, \end{cases}$$

is based on the Monaghan & Lattanzio (1985) SPH modelling, which was constructed guided by the accuracy, smoothness, and computational efficiency criteria. This spline-softened potential is equal to the Newtonian gravitational potential for distances greater than the softening length h , unlike the Plummer-softened potential used by NBODY-2, which converges slowly to the Newtonian one for long distances – see Fig. 1. In addition, we will refer to $\varepsilon_{eq} \equiv h/2.8$ as the Plummer-equivalent softening length for a given h set in GADGET-2. With this choice, the minimum of the GADGET-2 and the Plummer-softened gravitational potentials have the same depth at $r = 0$, as shown in Fig. 1.

All units adopted here are the same as those used internally and prompted by the simulation code, the so-called N -body units introduced by Hénon (1964), where the gravitational constant is $G = 1$, total mass $M = 1$, and total energy $E = -1/4$. This corresponds to a virial equilibrium radius $R = 1$ and rms velocity $V = \sqrt{2}/2$, and thus the crossing time $\tau_{cr} = 2R/V = 2\sqrt{2}$ – see Aarseth (2001).

3. ENTROPY ESTIMATORS

The entropy given by Eq. (7) is estimated using the data from the N -body simulation and translating the integral over the phase space into a sum over the N particles of the system (see Joe 1989; Hall & Morton 1993). Having an estimate $\hat{f}_i = \hat{f}(\vec{r}_i, \vec{v}_i, t)$ for the distribution

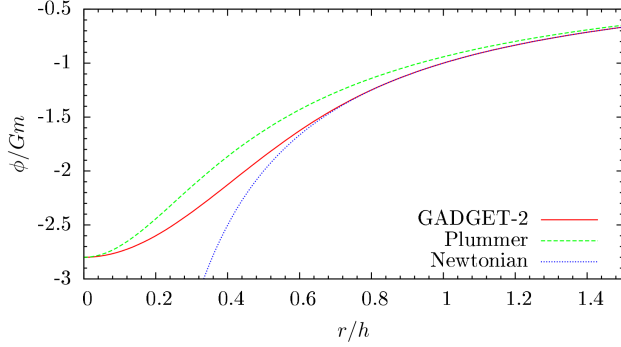


Figure 1. Comparison between the spline-softened GADGET-2, the Plummer-softened and the Newtonian gravitational potentials of a point mass. It was used here $h = 1.0$ and $\varepsilon = h/2.8$.

function f at the phase space position of each particle i , we estimate the entropy at each time as

$$\hat{S}(t) = -\frac{1}{N} \sum_{i=1}^N \ln \hat{f}_i. \quad (8)$$

The meaning and adequacy of this estimator becomes clear when we interpret Eq. (7) as the phase space average of $\ln f$. Assuming that the positions (\vec{r}_i, \vec{v}_i) of the particles in phase space are *independently distributed* with distribution f , it has been shown that this estimator converges in probability³ to the Shannon entropy given by Eq. (7) in the limit $N \rightarrow \infty$ (Joe 1989; Hall & Morton 1993). Note that assuming the validity of any dynamical equation for *one* typical particle as the effective equation for the macroscopic dynamics includes the assumption that the many-particle correlations do not participate in the effective dynamics, i.e., different particles typically evolve independently. Hence, seeing the phase space coordinates of particles as independent random variables is part of the hypothesis we are testing, namely, the validity of the Vlasov-Poisson equation. Fig. 2 shows the early (i.e. in a few dynamical time-scales) evolution of this estimation, with the following estimator for the distribution function.

We estimate the distribution function with the Kernel method (Silverman 1986), which models the distribution at a specified point as a sum of “bumps” centered at each one of the other particles:

$$\hat{f}_i = \hat{f}(\vec{r}_i, \vec{v}_i, t) = \frac{A}{N} \sum_{j=1}^N \frac{1}{h_j^6} K\left(\frac{D_{ij}}{h_j}\right), \quad (9)$$

³ This means that, given any fixed error $\varepsilon > 0$, the probability for the estimator to make an error larger than ε for the entropy associated to f tends to zero, as $N \rightarrow \infty$.

where D_{ij} is the phase-space distance (6-D) between particles i and j

$$D_{ij} = \sqrt{(\vec{r}_i - \vec{r}_j)^2 + (\vec{v}_i - \vec{v}_j)^2} \quad (10)$$

(using the dimensionless coordinates and velocities provided by the simulation code, i.e. in N-body units – see § 2) and $K\left(\frac{D_{ij}}{h_j}\right)$ is the kernel function, which determines the shape of the bumps. The parameter h_j , here allowed to vary for different particles (the adaptive kernel method), is the window width, and it determines the width of the bumps. This parameter introduces a certain degree of arbitrariness, analogous to that associated to the bin definitions of a histogram: it cannot be too small, thus introducing spurious and noisy substructures, nor too large, what would erase important information of the distribution. Choosing this parameters optimally corresponds to improving the convergence rate of the estimator. Here, we take h_j to be the phase space distance D_{jn} from particle j to its nearest neighbor (see §4.3), which is a standard choice. The normalization constant A is defined by the condition

$$A = \frac{1}{\int K(x) d^6x}, \quad (11)$$

x being a vector in 6-D, and we use the kernel

$$K\left(\frac{D_{ij}}{h_j}\right) = \frac{1}{(D_{ij}/h_j)^8 + 1}, \quad (12)$$

which implies $A = 8/(\sqrt{2}\pi^4) \approx 5.807 \times 10^{-2}$.

It is important to note that there is no need (if possible) to advocate any “coarse-grain” interpretation to our estimation of the distribution function, since our estimators are not based on phase-space averages of regions containing large numbers of particles. Instead, the distribution function at each phase-space position is estimated directly from the phase-space coordinates of each particle. In §4.3 we show the qualitative agreement for the entropy evolution estimated through the Kernel and Nearest Neighbor methods. For all the following calculations, we use the Kernel method instead of other methods such as the Nearest Neighbor (see §4.3) due to the good mathematical properties of the former at large dimensions. Indeed, in contrast to the Kernel method, the convergence of the Nearest Neighbor is only well-understood at dimension less than 3. Moreover, it is also possible to show that the Kernel estimation tends to the Nearest Neighbor estimation in the limit $h_j \rightarrow 0$.

3.1. Entropy production of a general process

Given the entropy estimator Eq. (8), we can calculate its time derivative and relate it to the relaxation term

as

$$\begin{aligned}\frac{d\hat{S}}{dt} &= -\frac{1}{N} \sum_{i=1}^N \frac{1}{\hat{f}_i} \frac{d\hat{f}_i}{dt} \\ &= -\frac{1}{N} \sum_{i=1}^N \frac{1}{\hat{f}_i} \left(\frac{\partial \hat{f}_i}{\partial t} \right)_X.\end{aligned}\quad (13)$$

Thus, the theoretical prediction for the entropy produced by any model through the relaxation term $(\partial f_i / \partial t)_X$ can be estimated with the simulation data, integrating $d\hat{S}/dt$ as

$$\hat{S}(t + \Delta t) = \hat{S}(t) + a \cdot \frac{d\hat{S}}{dt}(t) \Delta t \quad (14)$$

and fitting to the simulation data with 2 free parameters, $S_0 = S(0)$ and a . This can be compared to the entropy production obtained with the same data, Eq. (8), configuring a general method to test any theoretical transport equation, in particular the Fokker-Planck equation.

3.2. Fokker-Planck relaxation term

The Fokker-Planck approximation models the relaxation of the system as a result of the cumulative effects of many (2-body) weak encounters, with the energy change in each encounter being small. In the limit $N \rightarrow \infty$ the granularities of the potential due to the contribution of individual particles are erased and the system becomes collisionless, thus the relaxation due to the Fokker-Planck term is expected to be zero in this limit. However, in N -body simulations we necessarily use a finite number of particles, and consequently we need to estimate the contribution of the 2-body relaxation to the entropy increase.

The Fokker-Planck relaxation term is used below to estimate the 2-body relaxation contribution to the entropy production. Following standard procedures (Spitzer 1987; Binney & Tremaine 2008; Heggie & Hut 2003), we only consider diffusion in the velocity field, i.e., we consider a spatially homogeneous system, for which the general expression of the relaxation term is

$$\left(\frac{\partial f}{\partial t} \right)_{FP} = - \sum_{i=1}^3 \frac{\partial}{\partial v_i} (f \langle \Delta v_i \rangle) + \frac{1}{2} \sum_{i,j=1}^3 \frac{\partial^2}{\partial v_i \partial v_j} (f \langle v_i v_j \rangle), \quad (15)$$

where the indices i and j here refer to the 3 velocity components and not the particles as before. If the distribution function can be written as a function of the energy only (as it is assumed here), then after calculating the diffusion coefficients $\langle \Delta v_i \rangle$ and $\langle \Delta v_i \Delta v_j \rangle$, and assuming particles of equal masses, we get (see Spitzer 1987)

$$\left(\frac{\partial f}{\partial t} \right)_{FP} = \frac{4\pi\Gamma}{v^2} \frac{\partial}{\partial v} \left[f v^2 F_2 + \frac{v^3}{3} (F_4 + E_1) \frac{\partial f}{\partial v} \right], \quad (16)$$

where $\Gamma = 4\pi G^2 m^2 \ln \Lambda$ and

$$F_n(v) = \int_0^v \left(\frac{v'}{v} \right)^n f(v') dv' \quad (17)$$

$$E_n(v) = \int_v^\infty \left(\frac{v'}{v} \right)^n f(v') dv'. \quad (18)$$

The estimators associated to Eqs. (17) and (18) are given by

$$\hat{F}_{ni} = \frac{1}{N} \sum_{\substack{j=1 \\ v_j < v_i}}^N \left(\frac{v_j}{v_i} \right)^n \quad (19)$$

$$\hat{E}_{ni} = \frac{1}{N} \sum_{\substack{j=1 \\ v_j > v_i}}^N \left(\frac{v_j}{v_i} \right)^n, \quad (20)$$

and we see that

$$\frac{\partial \hat{F}_{ni}}{\partial v_i} = -\frac{n}{v_i} \hat{F}_{ni}(v_i) \quad (21)$$

$$\frac{\partial \hat{E}_{ni}}{\partial v_i} = -\frac{n}{v_i} \hat{E}_{ni}(v_i). \quad (22)$$

After some algebra, the estimator associated to Eq. (16) results in

$$\begin{aligned}\left(\frac{\partial \hat{f}}{\partial t} \right)_{FP} &= \frac{4\pi\Gamma}{3} \times \\ &\times \left[\left(3\hat{F}_2 - \hat{F}_4 + 2\hat{E}_1 \right) \frac{\partial \hat{f}}{\partial v} + v \left(\hat{F}_4 + \hat{E}_1 \right) \frac{\partial^2 \hat{f}}{\partial v^2} \right],\end{aligned}\quad (23)$$

where, from Eqs. (9), (10) and (12):

$$\frac{\partial \hat{f}_i}{\partial v_i} = -\frac{8}{N} \sum_{j=1}^N \frac{1}{h_j^8} \frac{(D_{ij}/h_j)^6}{[(D_{ij}/h_j)^8 + 1]^2} \left(v_i - \frac{\vec{v}_i \cdot \vec{v}_j}{v_i} \right) \quad (24)$$

and

$$\begin{aligned}\frac{\partial^2 \hat{f}_i}{\partial v_i^2} &= -\frac{8}{N} \sum_{j=1}^N \frac{1}{h_j^8} \frac{(D_{ij}/h_j)^4}{[(D_{ij}/h_j)^8 + 1]^2} \times \\ &\times \left\{ \frac{2}{h_j^2} \left[3 - \frac{8(D_{ij}/h_j)^8}{(D_{ij}/h_j)^8 + 1} \right] \cdot \left(v_i - \frac{\vec{v}_i \cdot \vec{v}_j}{v_i} \right)^2 + \left(\frac{D_{ij}}{h_j} \right)^2 \right\}.\end{aligned}\quad (25)$$

Substituting these expressions into Eq. (23), we can estimate at each time the contribution of the Fokker-Planck relaxation term to the entropy increase - see Fig. 3.

4. MAIN RESULTS

For our fiducial simulation run, we use $N = 10^5$ particles with a top-hat initial condition, i.e. a spherically symmetric and spatially homogeneous system, with an initial Maxwellian velocity distribution with velocity dispersion determined by the initial virial ratio set to $Q_0 = 0.5$, the value expected at equilibrium.

Fig. 2 shows the initial evolution of the entropy production $\hat{S}(t) - \hat{S}(0)$, as estimated by Eq. (8), with the help of Eqs. (9) to (12). The uncertainties were calculated as the standard deviation of 50 runs starting with different seeds for the random number generator. We clearly see that the entropy has a significant increase, accompanied by damping oscillations, in the dynamical time-scale indicated by the green dotted line, which corresponds to the time-scale during which the violent relaxation process is expected to occur – see § 1.

These oscillations could, naively, be interpreted as a violation of the second law of Thermodynamics, which predicts that the entropy must necessarily increase or be conserved. However, the observed global entropy increase is in accordance to this. What is apparently violated is the so-called H theorem, which predicts a monotonic increase of the H function *if the system's evolution is described by the Boltzmann equation*. This apparent violation of the H theorem is, however, a common feature of any system with an appreciable potential energy, as argued by Prigogine & Severne (1966); Jaynes (1971) – see also Romero-Rochin & González-Tovar (1997). As pointed out by those authors, these characteristic oscillations are the consequence of the conversion of kinetic to potential energy and vice-versa, a phenomenon which is known to occur during the collapse of self-gravitating systems. In fact, if we assume as a toy-model that the entropy of these systems has some similarity with that of ideal gases, depending on the volume V as $\propto \ln V$, the behavior seen in Fig. 2 can be associated to the system's macroscopic oscillations with collapse followed by some diffusive process and the correspondent expansion forming the external halo. Such entropy oscillations are also well-known in presence of memory terms in the effective dynamics.

4.1. Fokker-Planck approximation

We now verify if the entropy increase observed in Fig. 2 can be attributed to the 2-body relaxation as modelled by the Fokker-Planck approximation. For this, we use the estimators presented in §3 to plug Eq. (23) into Eq. (13) and calculate $d\hat{S}/dt$ at each time-step. This is then integrated with Eq. (14) and fit to the simulation data, with the parameter a being related to the unknown value of the Coulomb logarithm $\ln \Lambda$.

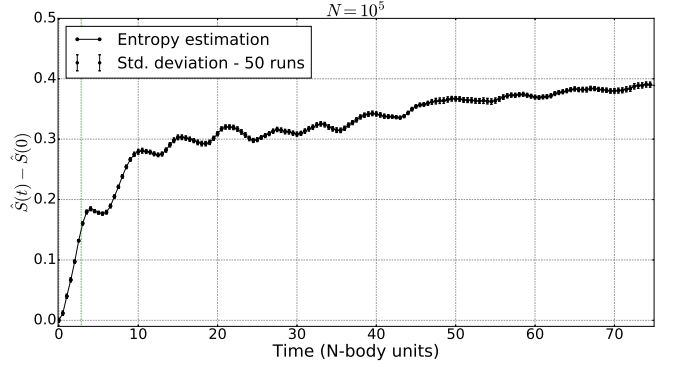


Figure 2. Entropy production estimation $\hat{S}(t) - \hat{S}(0)$, Eq. (8), for $N = 10^5$ particles starting with virial ratio $Q_0 = 0.5$, i.e. with the value expected at equilibrium. Uncertainties were calculated as the standard deviation of 50 runs starting with different seeds for the random number generator. The vertical green dotted line shows the dynamical (crossing) time-scale, $\tau_{dyn} = 2\sqrt{2}$, the time-scale in which violent relaxation is expected to occur. The significant entropy increase contrasts with the entropy conservation predicted by the Vlasov-Poisson equation.

Fig. 3 shows the entropy production estimation $\hat{S}(t) - \hat{S}(0)$ in the long-term evolution (t up to 2×10^3 in N -body units). After the fast increase at early times, as shown in Fig. 2, the entropy growth becomes slower and almost linear. The dashed curve shows the fit of the Fokker-Planck model when we consider all the data points. We clearly see that the model is not able to reproduce the data, and this is due to the high entropy production and oscillations at early times, during violent relaxation. On the other hand, if we restrict the fit to later times, say for $t \gtrsim 75$, we see a good agreement with the data, as shown by the solid line. Note that the apparently linear behaviour of the Fokker-Planck prediction is not put by hand, but it is a consequence of the non-trivial combination of the several terms in Eq. (23).

Thus, different from the early evolution, this long-term, almost linear, evolution of the entropy can then be attributed to the 2-body relaxation, in qualitative agreement with the collisional relaxation time-scale estimated by NBODY-6, indicated by the vertical solid line in Fig. 3.

4.2. Dependence on the number of particles

The distribution function estimation is expected to represent the true fine-grained distribution function and, in the limit $N \rightarrow \infty$, the distribution function of a collisionless system. One concern then is whether the number of particles used is enough for achieving convergence to this limit.

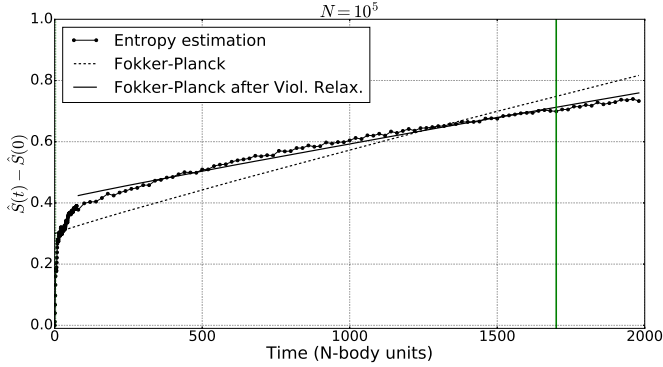


Figure 3. Entropy estimation for $N = 10^5$ particles (points). Note the difference in the range of the x-axis compared to Fig. 2. Dashed line: fit of the Fokker-Planck equation prediction, Eqs. (23) and (13), taking into account all the data points. The high entropy production at early stages prevent the model to adequately fit the (almost linear) long-term evolution of the entropy. Solid line: fit of the same model, but taking into account just the points for which $t > 75$. The model can fit the entropy evolution in this regime. Vertical green solid line: the half mass 2-body relaxation time-scale. The almost linear entropy increase in the long-term evolution can be explained by 2-body interactions as modeled by the Fokker-Planck equation, while the large increase associated to the violent relaxation at early times cannot be explained by 2-body interactions, i.e. it must be associated to a collective process, in agreement with the violent relaxation picture.

Fig. 4 shows the early entropy evolution for different numbers of particles (blue triangles for $N = 10^4$, black circles for $N = 10^5$ and red squares for $N = 10^6$). We see that the three curves have the same qualitative behaviour: a fast entropy increase, followed by damping oscillations. For $N = 10^4$, we still have significant noise deforming the oscillatory pattern, while for $N = 10^5$ and $N = 10^6$ the curves are smoother. Also, the curves for $N = 10^5$ and $N = 10^6$ are very similar and achieve the same value at $t \approx 75$, what indicates the convergence to the limit $N \rightarrow \infty$ for this early evolution.

In Fig. 5 we compare the long-term entropy evolution for these different numbers of particles (now with $N = 5 \times 10^5$ in place of $N = 10^6$), as well as the fit of the Fokker-Planck contribution. Again, we see that the Fokker-Planck equation is able to explain this evolution for $t \gtrsim 75$, but not the early evolution. Thus this long-term evolution can be attributed to the 2-body relaxation. Taking into account the estimate of the 2-body relaxation time-scale, Eq. (1), the fact that the slope of $S(t)$ is larger for decreasing number of particles shows that the 2-body relaxation is in fact more effective for a smaller number of particles, in agreement with the theoretical expectation: in the limit $N \rightarrow \infty$ we would

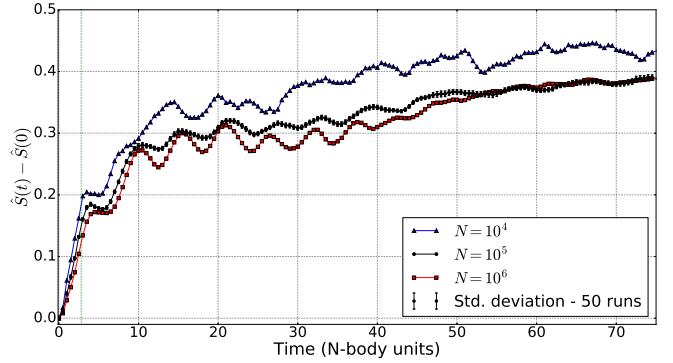


Figure 4. Entropy estimation for different numbers of particles as a function of time. Blue triangles for $N = 10^4$ particles, black circles for $N = 10^5$ and red squares for $N = 10^6$. The similarity between the curves for $N = 10^5$ and $N = 10^6$, mainly the fact that they evolve to the same value at $t \approx 75$, indicates the convergence to the evolution it would approach in the limit $N \rightarrow \infty$, i.e. to the collisionless limit.

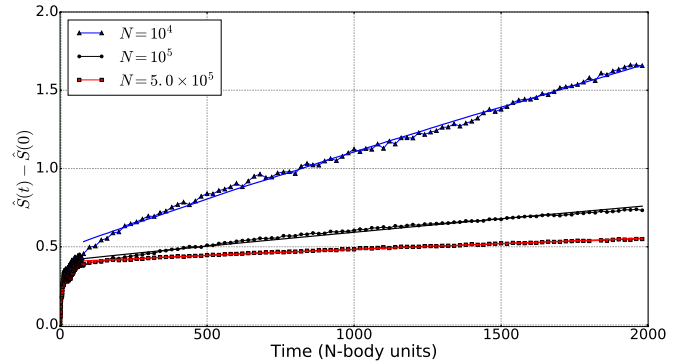


Figure 5. Entropy estimation for $N = 10^4$ (blue triangles), $N = 10^5$ (black circles) and $N = 5 \times 10^5$ (red squares). Similarly to Fig. 3 but now comparing different number of particles. The entropy increase during violent relaxation is similarly high for the three data sets. However, for the long-term evolution, during which we expect the 2-body relaxation to act, the slope of $S(t)$ is larger for a smaller number of particles N , in agreement with the theoretical expectation that the 2-body relaxation rate is larger for smaller N .

have a collisionless system and thus the slope of $S(t)$ predicted by the Fokker-Planck equation would be zero. The small value of the slope for $N = 5 \times 10^5$ reinforces this tendency.

With this long-term entropy evolution for varying numbers of particles, we can study the N -dependence of the collisional relaxation time-scale. A good global estimate of this quantity is the half-mass relaxation time-scale (Spitzer 1987)

$$\tau_{rh} \propto \frac{\sqrt{N}}{\ln \Lambda}. \quad (26)$$

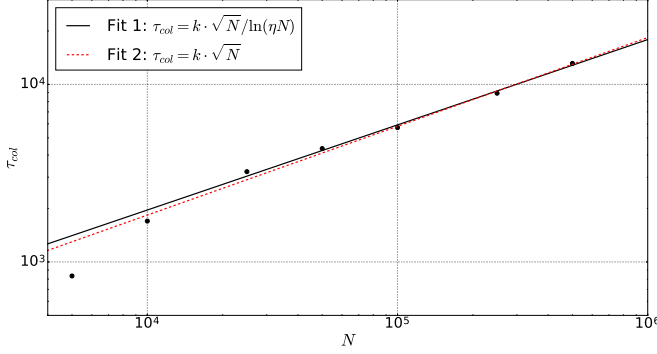


Figure 6. The collisional relaxation time-scale estimated with Eq.(27) with data from NBODY-6 for varying number of particles (points) and the fit of the theoretical half-mass relaxation time-scale, Eq. (26) – solid black line. Also shown the fit of the simpler function $\tau_{col} = k \cdot \sqrt{N}$ – dashed red line.

Regarding the definition of $\Lambda = b_{max}/b_0$, in principle, $b_{max} \rightarrow \infty$ and $b_0 \rightarrow 0$ what brings divergences in the Coulomb logarithm $\ln \Lambda$. These divergences are usually circumvented introducing a cut-off at some radius. For example, a common estimate is $b_{max} \approx R$ (Binney & Tremaine 2008), where R is the scale of the system’s size, while according to Chandrasekhar (1941, 1942); Chandrasekhar & von Neumann (1942); Kandrup (1980), one should use $b_{max} \approx N/R^{1/3}$ – see also Farouki & Salpeter (1982). On the other hand, b_0 is usually assumed to be the impact parameter associated to a 90° scatter, $b_0 \approx GM/(N\langle v^2 \rangle)$. Despite some controversy around the correct choice for b_{max} , most numerical tests favour $b_{max} \approx R$ – see Farouki & Salpeter (1982); Smith (1992); Farouki & Salpeter (1994); Theis (1998); Athanassoula et al. (2001) and §4.5 – which is the value used here.

According to the virial theorem, we have

$$\langle v^2 \rangle = \eta \frac{GM}{R},$$

where η is order unity and depends on the details of the mass distribution. Substituting in the expressions above, we have $b_0 = R/(\eta N)$ and $\ln \Lambda = \ln(\eta N)$ – see Farouki & Salpeter (1982) and references therein. We compare the N -dependence of the theoretical estimate for the collisional relaxation time-scale, Eq. (26), in Fig. 6. The empirical collisional relaxation time-scale is estimated as

$$\tau_{col} = \frac{1}{d\hat{S}/dt}, \quad (27)$$

where $d\hat{S}/dt$ is the angular coefficient of the fit of a straight line to the long-term entropy evolution, i.e. considering only data points with $t \gtrsim 75$.

Interestingly, the fit of Eq. (26) with the term $\Lambda = \eta N$ returns an extremely large value for the η parameter, in

practice implying a non-dependence of τ_{rh} on the term $\ln(\eta N)$ in the denominator of Eq. (26). Thus, besides Eq. (26), we also fit the simpler function $\tau_{col} = k \cdot \sqrt{N}$, which gives a slightly better fit, with $k = 6.49$, although still not perfect, specially for small N .

4.3. Nearest Neighbor vs Kernel method

We also estimate the distribution function $f(\vec{r}, \vec{v}, t)$ with the Nearest Neighbor method (see Silverman 1986), which is based on the following idea: sitting on particle i , we use Eq. (10) to calculate the (6-D) phase space distance D_{in} to particle n , its nearest neighbor, i.e. the smallest of the distances to all the other particles j , Eq. (10).

This distance is used to define a hyper-sphere of volume $\propto D_{in}^6$ centered on particle i . The estimation of the distribution function at the phase-space position of particle i is then

$$\hat{f}(\vec{r}_i, \vec{v}_i, t) \propto \frac{1}{D_{in}^6}, \quad (28)$$

i.e., it is the number of particles inside the sphere divided by its volume. In principle, this estimation must be normalized, but we use it just to estimate the entropy production $S(t) - S(0)$, for which additive constants cancel out.

Fig. 7 shows the early entropy evolution with the distribution function estimated from the two methods: the dots (triangles) show the estimation based on the Kernel (Nearest Neighbor) method. We see that, despite small differences (remember that the Kernel method tends to the Nearest Neighbor method for window width $h_j \rightarrow 0$), the two estimators provide the same result: the entropy has a fast monotonic increase up to the dynamical time-scale, followed by an increase with damping oscillations up to, at least, $t = 75$. After that, the entropy increases almost linearly – see Fig. 8, what can be attributed to the two-body relaxation, as seen before.

The similarity and smoothness of the curves obtained with different methods indicate that the features observed really represent the behaviour of the entropy during the evolution of the simulated system, and are not spurious effects associated to a particular method. It is interesting to note the similarity of the two methods for $N = 10^6$. Both the Kernel and the Nearest Neighbor estimators converge, independently of each other, to the same value (namely, the entropy of the considered distribution) as $N \rightarrow \infty$. Thus, this agreement suggests that the limit has been achieved.

4.4. Changing the initial conditions

We also studied what are the consequences of different initial conditions for the entropy evolution in two differ-

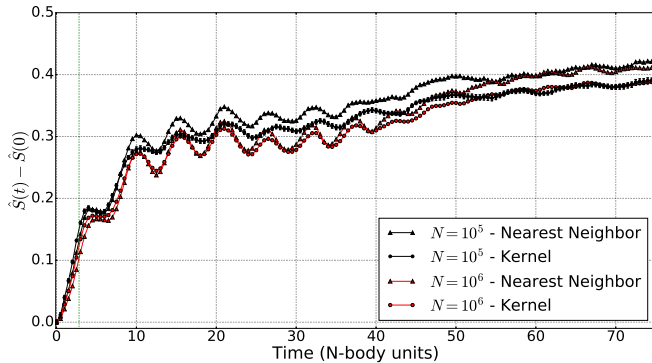


Figure 7. Entropy estimation for $N = 10^5$ (black) and $N = 10^6$ (red). The dots (triangles) show the entropy estimation obtained with the Kernel (Nearest Neighbor) estimated distribution function - see Eqs. (9) and (28). Despite little amplitude differences, the overall behavior of the estimation does not change for different estimators: the entropy increases accompanied by damping oscillations. For $N = 10^6$ the Kernel and Nearest Neighbor estimations are very similar, which also reinforces the idea of convergence to the limit $N \rightarrow \infty$. The dashed vertical line shows the dynamical time scale ($\tau_{dyn} = 2\sqrt{2}$), the scale in which the violent relaxation process is expected to occur.

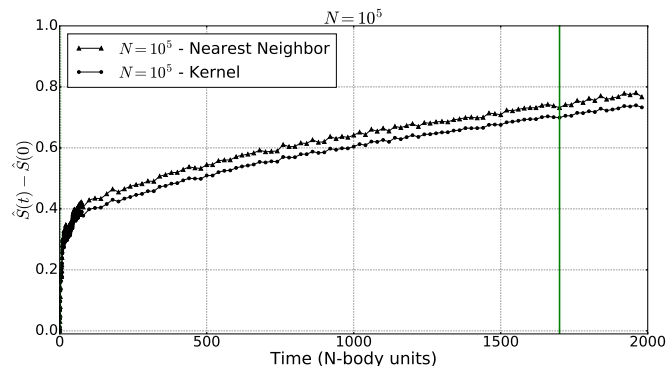


Figure 8. The same as Fig. 7, but now showing the long-term evolution of the entropy. We can see that both estimators provide the same behavior for the entropy, which increases almost linearly in the 2-body relaxation time-scale.

ent ways. First, we run the same simulations as before, with $N = 10^5$ particles and a top-hat initial spatial distribution with a Maxwellian velocity distribution, but now changing the initial virial ratio Q_0 . Remembering that the expected value at equilibrium is $Q = 0.5$ (the value used in the previous analyses), we set $Q_0 = 0.25$ in one run, which we call “cold” initial condition, and $Q_0 = 0.6$ in the other (“hot”). And second, in another run, we start the simulation with the Plummer density profile $\rho(x)$, which is given in dimensionless quantities by

$$\rho(x) = \frac{1}{(1 + x^2)^{5/2}},$$

x being the distance from the center. Although not being exactly the density profile expected at the end of the system’s evolution, it certainly represents a state closer to the equilibrium than the top-hat configuration used as the initial configuration in the other runs.

Fig. 9 shows the early entropy evolution for these configurations. We see that all three curves with a top-hat initial density profile and varying Q_0 show the same qualitative behaviour: a high entropy increase followed by damping oscillations, in the dynamical time-scale. On the other hand, this early entropy increase is significantly smaller (virtually negligible) for the initial Plummer density profile.

The most striking feature of this plot is the fact that when we start with initial conditions farther from equilibrium the entropy increase is higher, as we would expect. For the simulation starting with the Plummer density profile, which is close to the expected final state, the entropy production is almost zero. Therefore, the large entropy increase observed in the other curves probably cannot be attributed to any artificial numerical effect. Instead, as in the general idea of the entropy increase in any macroscopic system, it is the consequence of the choice of a particular initial state, very unlikely in comparison to the near-equilibrium state.

Fig. 10 shows the long-term evolution of the entropy for these simulations with different initial conditions. As in the other cases, the Fokker-Planck model can reproduce the almost linear entropy increase for $t \gtrsim 75$, but not for early times. While the entropy increase at early times depends crucially on the initial conditions, it is basically the same for the long-term evolution (same slope of $\hat{S}(t)$). In other words, collisional relaxation seems to depend just on N , but not on the initial conditions, while violent relaxation strongly depends on the initial conditions.

4.5. The role of the softening length

As mentioned in § 2, we also run simulations with the code NBODY-2, which makes use of a softening length in order to avoid close encounters and suppress the 2-body relaxation. Varying that parameter allows us to study the characteristic scales for different relaxation processes. Some particularly important scales in this respect are the system’s size $R \approx 1$ and the mean neighboring particle distance $\bar{D} = R/N^{1/3}$.

Fig. 11 shows the early evolution of the entropy for a simulation with $N = 10^5$ and the fiducial initial conditions, i.e. a top-hat with Maxwell velocity distribution and initial virial ratio $Q_0 = 0.5$, for different values of the NBODY-2 softening length ε . It is possible to see that the initial entropy increase is almost the same for

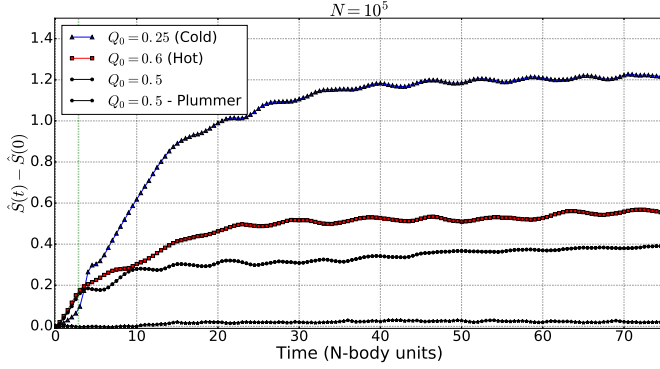


Figure 9. Entropy estimation for $N = 10^5$ particles and different initial conditions. Blue triangles: initial virial ratio $Q_0 = 0.25$ (“cold” initial condition). Red squares: $Q_0 = 0.6$ (“hot” initial condition). Black circles: the same as in Fig. 3, the case $Q_0 = 0.5$, i.e. it starts with the value expected at equilibrium. Black stars: initial Plummer density profile, which is close to the final configuration of the system. All these curves are consistent with the expectation that the farther from the equilibrium, the larger the entropy production. The dotted vertical line shows the dynamical time scale ($\tau_{dyn} = 2\sqrt{2}$), the scale in which the violent relaxation process is expected to occur.

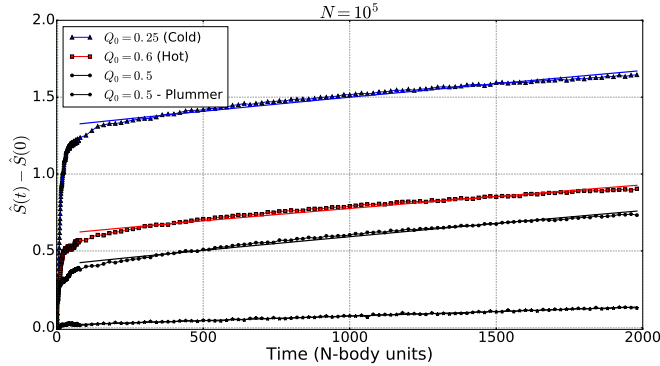


Figure 10. Same as Fig. 9, but now showing the long-term evolution.

all runs with $\varepsilon \leq 0.1$, suggesting that violent relaxation does not involve scales comparable to or smaller than the mean neighboring particle distance $\bar{D} \approx R/N^{1/3} \approx 0.02$. On the other hand, for $\varepsilon = 0.5$ and $\varepsilon = 1.0$, which are significantly larger than \bar{D} , we observe an important suppression in the early entropy production, indicating that the violent relaxation process really involves scales larger than \bar{D} . We notice that this is in accordance with recent mathematical results on effective dynamical equations for large Newtonian systems. See § 6 for further discussion.

The delayed entropy increase for these large values of ε can be interpreted as follows: with such high values of ε , the system starts evolving almost as if it was com-

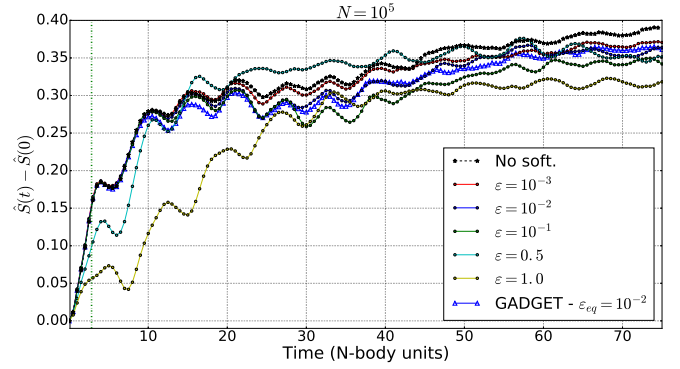


Figure 11. Entropy estimation for $N = 10^5$ particles obtained with NBODY-2 for different values of the softening length ε . The entropy production is suppressed just for softening length values comparable to the system size, i.e., considerably larger than the mean inter-particle distance $\bar{D} \approx R/N^{1/3} \approx 0.02$. Also shown the entropy obtained with GADGET-2 (blue void triangles) for a softening length $h = 2.8 \times 10^{-2}$, i.e. with a Plummer-equivalent softening length $\varepsilon_{eq} = 10^{-2}$, whose evolution is very similar to that of NBODY-2 with the same ε .

posed of non-interacting particles, for which the entropy should be constant. However, once the system expands, the typical distance between particles increases, “turning on” the interactions between particles with distances larger than ε , thus increasing the entropy.

We also simulate the evolution of one halo with the tree code GADGET-2, starting with exactly the same initial conditions as those of the previous simulations, and with a softening length $h = 2.8 \times 10^{-2}$, i.e. with a Plummer-equivalent softening length $\varepsilon_{eq} = 10^{-2}$ – see §2. The entropy evolution is shown as the blue open triangles in Fig. 11 and we see that it is very similar to that obtained with NBODY-2 and the same value of the softening length (blue points). Since these codes are based on very different integration techniques, this weakens the possibility of the entropy evolution observed being due to an artificial numerical relaxation, unless it is present in exactly the same way in both codes.

Fig. 12 shows the long-term entropy evolution and the fit of the Fokker-Planck model for different values of ε , but now with $N = 10^4$. The stars and the black dashed line represent the case obtained with NBODY-6, i.e. without softening length. Firstly, we can see that for $\varepsilon = 10^{-4} \approx R/N$ the entropy evolution is almost identical to that without softening length, i.e. scales smaller than this do not seem to be important for the 2-body relaxation. This confirms that $b_0 = b_{90} \approx GM/(N\langle v^2 \rangle) \approx R/N$ is a good choice for the minimum impact parameter for the gravitational scatterings – see § 3.2 and Farouki & Salpeter (1982). We clearly see that larger values of the softening length

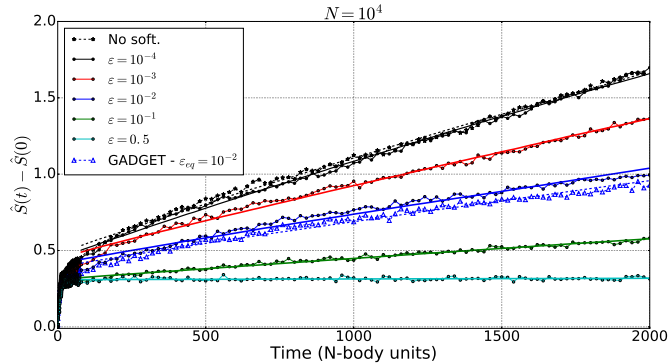


Figure 12. Long-term evolution of the entropy estimation for $N = 10^4$ particles obtained with NBODY-2 for different values of the softening length ε . As expected, the suppression of collisional relaxation is larger for larger ε , saturating just at scales of the size of the system ($R \approx 1.0$). This favours $b_{max} = R$ – see § 3.2. For $\varepsilon = 10^{-4} \approx R/N$, the entropy evolution is identical to that without softening length (stars and black dashed line), in agreement with $b_0 = b_{90} \approx GM/(N\langle v^2 \rangle) \approx R/N$. Also shown the entropy obtained with GADGET-2 (blue open triangles) for a softening length $h = 2.8 \times 10^{-2}$, i.e. with a Plummer-equivalent softening length $\varepsilon_{eq} = 10^{-2}$, whose evolution is very similar to that of NBODY-2 with the same ε .

increasingly suppress the 2-body relaxation, even for $\varepsilon > \bar{D} = R/N^{1/3} \approx 0.05$. This indicates that scatterings involving distances $> \bar{D}$ seem to be important for the 2-body relaxation, favoring $b_{max} = R$, in contrast to $b_{max} = \bar{D}$ as predicted by some authors – see Farouki & Salpeter (1994), although more detailed analysis, with larger N , would be necessary. It is also interesting to note that for $\varepsilon = 0.5$, i.e. a value slightly smaller than the scale of the system $R \approx 1$, the 2-body relaxation is almost completely suppressed, while the entropy increase produced by violent relaxation is still there, reinforcing the idea that it is associated to a collective effect, involving scales significantly larger than the mean neighboring particle distance \bar{D} .

In Fig. 12 the blue open triangles represent the entropy evolution obtained from GADGET-2 with $N = 10^4$, the same initial conditions as before and with a softening length $h = 2.8 \times 10^{-2}$, i.e. with a Plummer-equivalent softening length $\varepsilon_{eq} = 10^{-2}$ – see §2. Also shown is the fit of the Fokker-Planck model (dashed blue line), from which we see that the 2-body relaxation is slightly more suppressed with GADGET-2 than with NBODY-2 with equivalent softening lengths (see also Fig. 13), but their overall evolutions are very similar.

In Fig. 13 we show the collisional relaxation time scale estimated with Eq. (27) obtained with NBODY-2 for different values of the softening length ε . The solid curve is the best fit of the expression $\tau_{col} = a + b \cdot \sqrt{\varepsilon} \cdot e^{c\varepsilon}$,

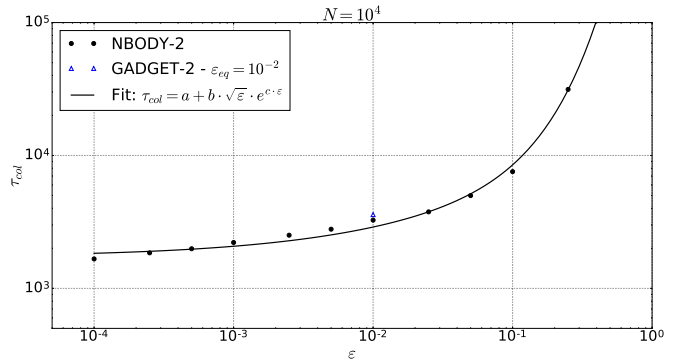


Figure 13. The collisional relaxation time-scale estimated with Eq. (27) for $N = 10^4$ as a function of the softening length ε . Also shown the fitting function (solid line). The blue open triangle represents the collisional time scale obtained with GADGET-2 and $\varepsilon_{eq} = 10^{-2}$.

with $a = 1727$, $b = 10907$ and $c = 6.74$. The blue open triangle shows the collisional relaxation time scale obtained with GADGET-2 for $\varepsilon_{eq} = 10^{-2}$, as in Fig. 12, which is slight higher than that obtained with NBODY-2 for equivalent softening lengths.

5. CONCLUSIONS

As discussed in §1, the validity of the Vlasov-Poisson equation implies the conservation of quantities defined by Eq. (4), for any functional $s[f]$ – see Tremaine et al. (1986). Conversely, non-conservation of any such quantity, like the Shannon entropy, implies the non-validity of the Vlasov-Poisson equation. In this paper, through the use of N -body simulations, we estimate the entropy at each time step, following its time evolution in order to test the validity of the Vlasov-Poisson equation for a collisionless self-gravitating system during violent relaxation.

Our results show a clear separation between the two relevant time scales: during the early stages, in the dynamical time scale, the entropy has a significant increase accompanied by damping oscillations – see Fig. 2. This is the time scale in which the violent relaxation process is known to operate, the relaxation being associated to the typical particle interaction with the time-changing collective gravitational potential. Instead of representing an exceptional situation, the oscillations observed reinforce the reliability of our results, since they are typical of systems with considerable potential energy, as pointed out by Prigogine & Severne (1966); Jaynes (1971); Romero-Rochin & González-Tovar (1997). Moreover, Jaynes (1971) argues that the fact the “H” function is not monotonic can be associated to the non-validity of the hypothesis of molecular chaos, which is of fundamental importance in the derivation of the Vlasov-Poisson

equation through the BBGKY hierarchy, a possibility also suggested by [Beraldo e Silva et al. \(2014\)](#).

On the other hand, in the collisional relaxation time scale the entropy increases almost linearly. In order to verify if this entropy increase can be produced by 2-body relaxation, we estimate the contribution of the Fokker-Planck model to the entropy increase, Eqs. (13) and (23). Fig. 3 shows that this is the case indeed: if we restrict the fit to points after the early stages, say for $t \gtrsim 75$, the Fokker-Planck model can reproduce the almost linear entropy increase. However, if we include all the data points, we have a poor fit, due to the large entropy increase and oscillations at early stages, which cannot be reproduced by the Fokker-Planck model.

Regarding the number of particles, we see in Fig. 4 that the early evolution of the entropy is qualitatively similar for $N = 10^4$, $N = 10^5$ and $N = 10^6$. The more irregular appearance of the data points for $N = 10^4$ can be attributed to shot noise due to the relatively small number of particles, while for $N = 10^5$ and $N = 10^6$ the curves are pretty smooth.

We note that the oscillation amplitudes are larger for $N = 10^6$ in comparison to $N = 10^5$. This can be interpreted as follows: the 2-body relaxation, although globally negligible for the entropy increase already for $N = 10^5$, can still act to destroy the coherent oscillatory pattern, smoothing out the curve, while for $N = 10^6$ the 2-body relaxation has even less effect, allowing the presence of coherent oscillations for a longer time period. This also reinforces the idea that the convergence to the limit $N \rightarrow \infty$, i.e. to the collisionless regime, has been achieved.

The entropy long-term evolution for different particle numbers allows us to study the N -dependence of the collisional relaxation time-scale. We observe a reasonable agreement with the theoretical half-mass relaxation time-scale, although a fit of a simpler expression without the Coulomb logarithm seems preferable.

We also studied the impact of different initial conditions on the entropy evolution. The general conclusion is that the entropy increase is higher for initial conditions farther from the equilibrium state. In particular, starting the simulation with a Plummer density profile (which is the closest to the equilibrium among our sets of initial conditions) we see a negligible entropy increase. This is in agreement with the general idea behind the statistical interpretation of the second law of Thermodynamics: that the systems evolve to the most probable state and that the entropy increases due to the particular choice of a initial state which is very unlikely in comparison to the equilibrium state. The fact that we observe a negligible entropy increase in the case of the

Plummer initial density profile also weakens the possibility that the entropy increase observed in the other runs is being produced by some artificial, numerical relaxation. Another interesting observation is that while the effectiveness of violent relaxation depends crucially on the initial conditions, the 2-body relaxation seem to depend only on the number of particles N .

The variation of the softening length ε in the simulations generated with NBODY-2 allowed us to study some characteristic scales both for the violent and collisional relaxation. Our results indicate that violent relaxation involves large scales as compared to the mean neighboring particle distance. On the other hand, our results seem to indicate that the important scales for the collisional relaxation are within the interval $R/N \leq b \leq R$.

We also find that the entropy evolution obtained with the tree code GADGET-2 is very similar to that obtained with NBODY-2 for equivalent softening lengths, despite the fact these codes involve different integration techniques. This reinforces the idea that the entropy evolution observed is not a numerical effect, but a real physical effect.

In conclusion, our results show that during violent relaxation there is a significant entropy increase despite the prediction of the Vlasov-Poisson equation of entropy conservation. Moreover, this entropy increase cannot be described by the 2-body relaxation as modeled by the Fokker-Planck equation. In fact, under the assumption that the convergence to the limit $N \rightarrow \infty$ has been achieved (which seems to be the case), this entropy increase cannot be attributed to any 2-body relaxation process, and must be associated to a collective effect, which is the original idea behind the violent relaxation process.

These results allow us to conclude that the Vlasov-Poisson equation is not valid for collisionless self-gravitating systems during violent relaxation, resurrecting the arrow of time in the collapse of these systems.

6. FINAL REMARKS

The disagreement between the assumption of validity of the (time-reversible) Vlasov-Poisson equation and the (macroscopically time-irreversible) scenario of violent relaxation has been already called the “fundamental paradox of stellar dynamics” ([Ossipkov 2006](#)). Furthermore, the inherently chaotic behavior of N -body self-gravitating systems (regarding the exponential divergence of close trajectories) seems to be in conflict with the Hamiltonian evolution driven by the Vlasov-Poisson equation ([Hemsendorf & Merritt 2002](#)). See also [Kandrup \(1998\)](#); [Merritt \(2005\)](#) for critical dis-

cussions relating the N -body problem and the Vlasov-Poisson equation.

In fact, this uncomfortable situation can be seen in several works. According to Madsen (1987), “to reach the predicted most probable final state, the system may have to break Liouville’s theorem [Vlasov-Poisson equation]”. Shu (1987) argues that “while Liouville’s theorem [Vlasov-Poisson equation] does apply on a microscopic level, it must necessarily be violated on a macroscopic level if the concept of violent relaxation is to have sensible meaning”. According to Kandrup (1998), “The N -body problem appears to be chaotic on a time scale τ_{cr} , but the flow associated with the CBE [Vlasov-Poisson equation] is often integrable or near-integrable in the sense that many or all of the characteristics are regular, i.e., non chaotic. So what do the (often near-integrable) CBE characteristics have to do with the true (chaotic) N -body problem? (...) The correct answer to the question raised above (...) is not completely clear. What does, however, seem apparent from the preceding is that, even for very large N , true N -body trajectories could differ significantly from CBE characteristics”. Hemsendorf & Merritt (2002) claim that “if the rate of growth of small perturbations remains substantial even for large N , there would be an important sense in which the CBE does not correctly describe the behavior of N -body systems”. Finally, Bindoni & Secco (2008) say that: “Any further relaxation of the system should be therefore considered in terms of the coarse-grained phase-space density which, as we have seen, would yield results different from the predictions based on the initial fine-grained phase-space density. This is a worrying aspect of these theories (...). The predictions of the theory, based on the fine-grained density, will then give a wrong result”.

In this work, we have argued that the apparent paradox disappears once we abandon the assumption of validity of the Vlasov-Poisson equation during violent relaxation. In our view, this assumption is due to an oversimplifying treatment of the very singular, at large and small distances, gravitational (Coulomb) potential: The first mathematically rigorous derivations of Vlasov equation⁴ can be found, e.g., in Neunzert & Wick (1974); Braun & Hepp (1977); Dobrushin (1979); Neunzert (1984). Rather than the Vlasov-Poisson equation, Neunzert & Wick (1974); Braun & Hepp (1977); Dobrushin (1979); Neunzert (1984); Spohn (2011) consider models with *continuous* and *bounded* forces. In particular, these forces

are not diverging at small inter-particle distances D , in contrast to gravitational (Coulomb) forces. In the last few years progress has been made in treating mean field limits for forces which are singular at small distances up to but not including the Coulomb case. Jabin & Hauray (2011) discusses forces diverging as $\sim D^{-\alpha}$ with $\alpha < d - 1$ in $d \geq 3$ dimensions. More precisely, in the case $1 < \alpha < d - 1$, a softening length of order $N^{-\frac{1}{2d}}$ is assumed in the derivation of the Vlasov equation from the N -body problem (Jabin & Hauray 2011). If $\alpha < 1$ no positive softening length is needed in the proof. Kiessling (2014) managed to prove a result including the Coulomb singularity under the assumption of an (uniform in N) a priori bound on the microscopic forces. However, whether it is satisfied for generic initial data or not, remains an open problem (Kiessling 2014). Boers & Pickl (2016) improved the result of Jabin & Hauray (2011) in the sense that the softening length used is of order $N^{-\frac{1}{d}}$, but still α has to be strictly smaller than $d - 1$ (and the Coulomb case is again not included). Recently, Lazarovici (2016); Lazarovici & Pickl (2015) extended the method of Boers & Pickl (2016) to include the Coulomb singularity, in 3 dimensions, aiming at a microscopic derivation of the Vlasov-Poisson dynamics. As in Jabin & Hauray (2011), a strictly positive softening length is needed, at fixed N . It can be chosen, as shown in Lazarovici & Pickl (2015), of order $N^{-\beta}$ with $\beta < \frac{1}{3}$.

These mathematical results suggest that inter-particle interactions taking place up to distances that are large compared to the mean neighboring particle distance \bar{D} , but small compared to the size of the whole system, could prevent the Vlasov-Poisson equation from being the effective macroscopic equation governing the evolution of large gravitational systems. The numerical results on the entropy production discussed here point in the same direction, indicating that violent relaxation involves scales significantly larger than \bar{D} – see Fig. 11.

We recall that even though a transport equation refers to the coordinates of one particle, it is not an equation of motion for some specific, randomly chosen, particle or fluid element. Instead, it statistically expresses the evolution of the system as a whole, referring to the coordinates of a statistical entity, the typical (or test) particle. As a result, it captures the influence of collective effects, which cannot be achieved using the equations of motion for a single particle. We should also mention that the right hand side of a transport equation is associated to any process relaxing the system, which only in the case of a molecular gas is necessarily realized by collisions, i.e. 2-body interactions. This point is particularly important for a system with long-range interac-

⁴ For a general overview of the topic, we refer the reader to the monograph Spohn (2011).

tions, which can relax even if it is collisionless⁵. In fact, taking the presence of chaotic motions as a diagnostic of relaxation, it is interesting to remember that N -body self-gravitating systems can exhibit large (and increasing as $\ln N$) rates of growth of small perturbations, even for large N – see Hemsendorf & Merritt (2002). In other words: these systems seem to be more chaotic for larger N , i.e. when they approach the collisionless regime – see also Kandrup & Sideris (2003).

The original statistical meaning of the distribution function seems to be frequently neglected, and in our opinion, the standard view of the necessity of a “coarse grained” interpretation for the macroscopic evolution of the system serves to introduce this statistical meaning. This “coarse grained” interpretation also seems to be a reminiscent of discussions regarding the differences between Gibbs’s and Boltzmann’s definitions of entropy (Lebowitz 1993a,b; Jaynes 1965; Goldstein 2001). The former makes reference to the N -particle distribution function $f^{(N)}$, which is subject to Liouville’s equation $df^{(N)}/dt = 0$, and thus is conserved, while the latter is defined in terms of the one-particle distribution function f , and evolves in time. According to Jaynes (1965), “since the Gibbs H is dynamically constant, one has resorted to some kind of coarse-graining operation, resulting in a new quantity \bar{H} , which tends to decrease (...). Mathematically, the decrease in \bar{H} is due only to the artificial coarse-graining operation and it cannot, therefore have any physical significance (...). The difference be-

tween H and \bar{H} is characteristic, not of the macroscopic state, but of the particular way in which we choose to coarse-grain. Any really satisfactory demonstration of the second law must therefore be based on a different approach than coarse-graining”. As we can see, this “coarse grained” interpretation can be necessary (although being subject to criticism) when we adopt the Gibbs definition of entropy, i.e. in terms of $f^{(N)}$. However, if we adopt the Boltzmann definition in terms of f , as done in this work, this is not necessary once we recognize the statistical content of the distribution function and abandon the assumption of validity of the Vlasov-Poisson equation during violent relaxation.

ACKNOWLEDGEMENTS

We are very grateful to S. Aarseth for all the help with the codes NBODY-6 and NBODY-2. We also thank Jean-Bernard Bru and Roberto Venegeroles for discussions. This work has made use of the computing facilities of the Laboratory of Astroinformatics (IAG/USP, NAT/Unicsul), whose purchase was made possible by the Brazilian agency FAPESP (grant 2009/54006-4) and the INCT-A. We are specially grateful to Carlos Paladini, without whom this work would not have been possible. LBeS. and ELDP are supported by FAPESP. LSJ acknowledges support by FAPESP (2012/00800-4) and CNPq. ML is also partially supported by FAPESP and CNPq. WdeSP is partially supported by FAPESP, CNPq and the Spanish Ministry of Economy and Competitiveness (grant SEV-2013-0323).

REFERENCES

- Aarseth, S. 1999, in Bulletin of the American Astronomical Society, Vol. 31, AAS/Division of Dynamical Astronomy Meeting, 1226
- Aarseth, S. J. 2001, New Astronomy, 6, 277
- . 2003, Gravitational N-Body Simulations, 430
- Ahmad, A., & Cohen, L. 1973, JCP, 12, 389
- Athanassoula, E., Vozikis, C. L., & Lambert, J. C. 2001, AA, 376, 1135
- Balescu, R. 1975, Equilibrium and Non-Equilibrium Statistical Mechanics (John Wiley & Sons)
- Beraldo e Silva, L., Lima, M., Sodr , L., & Perez, J. 2014, Phys. Rev. D, 90, 123004
- Bindoni, D., & Secco, L. 2008, NAR, 52, 1
- Binney, J., & Tremaine, S. 2008, Galactic Dynamics - Second Edition (Princeton University Press)
- Boers, N., & Pickl, P. 2016, JSP, 164, 1
- Braun, W., & Hepp, K. 1977, CMP, 56, 101
- Brush, S. 1976, The kind of motion we call heat: a history of the kinetic theory of gases in the 19th century No. vol. 6,n.2 (North-Holland Pub. Co.)
- Chandrasekhar, S. 1941, ApJ, 94, 511
- . 1942, Principles of stellar dynamics
- Chandrasekhar, S., & von Neumann, J. 1942, ApJ, 95, 489
- Colombi, S., Sousbie, T., Peirani, S., Plum, G., & Suto, Y. 2015, MNRAS, 450, 3724
- Dobrushin, R. L. 1979, FAIA, 13, 115
- Eftymiopoulos, C., Voglis, N., & Kalapotharakos, C. 2007, in Lecture Notes in Physics, Vol. 729, Topics in Gravitational Dynamics, ed. D. Benest, C. Froeschle, & E. Lega (Springer Berlin Heidelberg), 297–389
- Ehrenfest, P., & Ehrenfest, T. 1959, The conceptual foundations of the statistical approach in mechanics (Cornell University Press)

⁵ This is the reason why we prefer not to call Eq. (2) the “collisionless Boltzmann equation” as recommended by H  non (1982).

- Farouki, R. T., & Salpeter, E. E. 1982, *ApJ*, 253, 512
— . 1994, *ApJ*, 427, 676
- Goldstein, S. 2001, in *Chance in Physics*, Vol. 574, 39
- Hahn, O., & Angulo, R. E. 2016, *MNRAS*, 455, 1115
- Hall, P., & Morton, S. C. 1993, *AISM*, 45, 69
- Heggie, D., & Hut, P. 2003, *The Gravitational Million-Body Problem: A Multidisciplinary Approach to Star Cluster Dynamics*
- Hemsendorf, M., & Merritt, D. 2002, *ApJ*, 580, 606
- Hénon, M. 1964, *Annales d'Astrophysique*, 27, 83
- Hénon, M. 1982, *AAP*, 114, 211
- Horst, E. 1993, *MMAS*, 16, 75
- Jabin, P.-E., & Hauray, M. 2011, *arXiv:1107.3821*
- Jaynes, E. T. 1965, *Am. J. Phys.*, 33, 391
— . 1971, *PRA*, 4, 747
- Joe, H. 1989, *AISM*, 41, 683
- Kandrup, H. E. 1980, *Physics Reports*, 63, 1
— . 1990, *Physica A*, 169, 73
- Kandrup, H. E. 1998, *Annals NY Academy of Sciences*, 848, 28
- Kandrup, H. E., Mahon, M. E., & Smith, Jr., H. 1993, *Astronomy and Astrophysics*, 271, 440
- Kandrup, H. E., & Sideris, I. V. 2001, *PRE*, 64, 056209
— . 2003, *ApJ*, 585, 244
- Kandrup, H. E., Vass, I. M., & Sideris, I. V. 2003, *MNRAS*, 341, 927
- Kiessling, M. K.-H. 2014, *JSP*, 155, 1299
- King, I. 1962, *AJ*, 67, 471
- Lazarovici, D. 2016, *CMP*, 347, 271
- Lazarovici, D., & Pickl, P. 2015, *ArXiv e-prints*, *arXiv:1502.04608*
- Lebowitz, J. L. 1993a, *Physics Today*, 46, 32
— . 1993b, *Physica A*, 194, 1
- Levin, Y., Pakter, R., Rizzato, F. B., Teles, T. N., & Benetti, F. P. C. 2014, *Physics Reports*, 535, 1
- Lifshitz, E. M., & Pitaevskii, L. P. 1980, *Physical Kinetics* (ButterworthHeinemann)
- Lions, P. L., & Perthame, B. 1991, *IM*, 105, 415
- Lynden-Bell, D. 1967, *MNRAS*, 136, 101
- Madsen, J. 1987, *ApJ*, 316, 497
- Makino, J., & Aarseth, S. J. 1992, *PASJ*, 44, 141
- Merritt, D. 1999, *PASP*, 111, 129
— . 2005, *Annals NY Acad. of Sciences*, 1045, 3
- Merritt, D., & Valluri, M. 1996, *ApJ*, 471, 82
- Monaghan, J. J., & Lattanzio, J. C. 1985, *AAP*, 149, 135
- Neunzert, H. 1984, *Lecture Notes in Mathematics*, Berlin Springer Verlag, 1048, 60
- Neunzert, H., & Wick, J. 1974, *ZAMM*, 54, 194
- Nitadori, K., & Aarseth, S. J. 2012, *MNRAS*, 424, 545
- Ossipkov, L. P. 2006, *AAT*, 25, 123
- Padmanabhan, T. 1990, *Physics Reports*, 188
- Pfaffelmoser, K. 1992, *JDE*, 95, 281
- Prigogine, I., & Severne, G. 1966, *Physica*, 32, 1376
- Romero-Rochin, V., & González-Tovar, E. 1997, *JSP*, 89, 735
- Saslaw, W. C. 1987, *Gravitational Physics of Stellar and Galactic Systems*
- Schaeffer, J. 1991, *CPDE*, 16, 1313
- Shu, F. H. 1978, *ApJ*, 225, 83
- Shu, F. H. 1987, *ApJ*, 316, 502
- Silverman, B. W. 1986, *Density estimation for statistics and data analysis*
- Smith, Jr., H. 1992, *ApJ*, 398, 519
- Spitzer, L. 1987, *Dynamical evolution of globular clusters*
- Spohn, H. 2011, *Large Scale Dynamics of Interacting Particles, Theoretical and Mathematical Physics* (Springer Berlin Heidelberg)
- Springel, V. 2005, *MNRAS*, 364, 1105
- Theis, C. 1998, *AA*, 330, 1180
- Tremaine, S., Hénon, M., & Lynden-Bell, D. 1986, *MNRAS*, 219, 285
- Valluri, M., & Merritt, D. 1998, *ApJ*, 506, 686
- Yoshikawa, K., Yoshida, N., & Umemura, M. 2013, *APJ*, 762, 116